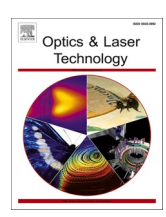


Contents lists available at ScienceDirect

Optics and Laser Technology

journal homepage: www.elsevier.com/locate/optlastec





Femtosecond laser direct weaving bioinspired superhydrophobic/ hydrophilic micro-pattern for fog harvesting

Jingzhou Zhang, Yuanchen Zhang, Jiale Yong, Xun Hou, Feng Chen

State Key Laboratory for Manufacturing System Engineering and Shaanxi Key Laboratory of Photonics Technology for Information, School of Electronic Science and Engineering, Xi'an Jiaotong University, Xi'an 710049, PR China

ARTICLE INFO

Keywords:
Fog harvesting
Femtosecond laser
Superhydrophobic
Desert beetle

ABSTRACT

In this paper, we directly built hybrid superhydrophobic/hydrophilic micro-patterns on Ti surfaces via femto-second laser microfabrication. After dark storage, superhydrophobic TiO_2 micro/nanostructures were formed on laser-scanned areas while un-scanned areas remained intrinsic hydrophilicity. The as-prepared Ti surface enhanced the water-collection efficiency by nearly 100% compared to the untreated one. Furthermore, the femtosecond laser direct weaved micro-pattern exhibited a fast processing speed and the whole process did not need any chemical modification. Our study provides a novel strategy to ameliorate the water shortage in the future.

1. Introduction

Due to environmental pollution, climate change and population growth, the shortage of water recourses is increasingly serious around the world. Statistically, the per-capita average of freshwater has decreased by more than 20% in the past 20 years [1–4]. To survive in an arid environment, desert beetles have evolved a unique property to capture and collect water mist from the atmosphere, which is resulted from its hybrid hydrophobic/hydrophilic back [5,6]. Water mist is transported by wetting gradient force from hydrophobic area to hydrophilic area and collected by hydrophilic micro-humps. Recently, inspired by nature, building a hybrid micro-pattern for water harvesting is found to be an important way to ease water shortages [7–11]. The key role to realize water harvesting with high efficiency is building wetting gradient or structural gradient on a micro-scale [12–19].

Femtosecond laser microfabrication was widely utilized to control the surface wettability and topography owing to its good consistency, high precision, and negligible heat-affected zone [20–29]. Various micro-patterned surfaces were designed by femtosecond laser for highly efficient fog collection [30–34]. For instance, by laser scanning, laser drilling, and modification of fluoride. Wu et al. prepared hydrophobic/hydrophilic Janus structures with micropore arrays on Al membranes for water harvesting [32]. Zhong et al. fabricated a laser-induced hybrid superhydrophilic/superhydrophobic venation network [33], which achieves the self-driven transportation and collection of water on a large

surface. Guo et al. reported a physicochemical hybrid method to form hydrophobic/hydrophilic surfaces [34], which includes femtosecond laser structuring, hydrothermal treatment, and PDMS modification. Water harvesting could be realized even under low humidity. Although water collection efficiency was significantly improved by current works, the fabrication process was still lengthy and complicated. Meanwhile, to lower the surface free energy, chemical treatment such as fluoride was frequently used. It not only contaminated the environment during production but also caused the secondary pollution of collected water. A simple and direct way to build hydrophobic/hydrophilic micro-pattern without any chemical modification is still challenging.

In this study, inspired by desert beetles, superhydrophobic/hydrophilic micro-patterns were directly formed on Ti surfaces for water harvesting (Fig. 1). Femtosecond laser irradiation not only built micro/nanostructures but also ${\rm TiO_2}$ layer on Ti surface. After femtosecond laser weaving process and dark storage, the as-prepared surface was consist of laser-ablated ${\rm TiO_2}$ microgroove with superhydrophobic property and untreated Ti square array with hydrophilicity. By adjusting the ratio of laser irradiated area, the as-prepared surface exhibited high efficiency for water collection. Moreover, the whole fabrication process was green and efficient, which might provide a new insight for ameliorating the water shortages.

E-mail address: chenfeng@mail.xjtu.edu.cn (F. Chen).

^{*} Corresponding author.

2. Experimental section

Fabrication of superhydrophobic/hydrophilic micro-pattern on Ti sheets. Firstly, Ti sheets were applied to collect water owing to their controllable wettability and environment friendliness [35]. The size of each Ti sheet was $2.5 \times 2.5 \times 0.1$ cm³ and the purity of the Ti sheet was 99.7%. Secondly, TiO₂ micro-patterns on Ti surfaces were built by lineby-line femtosecond laser microfabrication. The femtosecond laser was generated from a Ti: sapphire regenerative amplifier (Institute of Physics, CAS, Harmonic Laser). The center wavelength was 800 nm. The repetition rate was 1000 Hz and its pulse width was 35 fs. The femtosecond laser beam was focused onto Ti sheets by a microscope objective lens (10 \times , NA = 0.30, Nikon). The diameter of the laser beam is about 2 mm and the focal length is 16 mm. So that the focal spot size can be calculated as 4 μ m. The single laser pulse energy was about 300 μ J. The irradiated speed was set at 5000 µm/s and the distance of adjacent irradiated lines was set at 20 μm . To weave square array patterns, the Ti sheets were selectively ablated and controlled by a pre-set computer program. As shown in Fig. 1, the gray mesh pattern denoted the laserirradiated stripe, while the blue domain was the untreated area. The period (*P*) of the mesh array was programmed to 300 μ m (*P* = 300 μ m). The width (W) of each laser irradiated stripe is consists of three laser irradiated lines. Hence, the length (L) of the untreated square was controlled as 300 μ m – 20 μ m \times 3 = 240 μ m (L = 240 μ m) and the ratio of the laser structured area was calculated as 36%. Thirdly, the resultant sheets were stored in an opaque oven (Figure S1, Supporting Information) at 100°C for 24 h to dark storage. After that, the laser-irradiated area changed into superhydrophobicity while the wettability of the untreated area is still hydrophilic. Finally, superhydrophobic/hydrophilic micro-patterns on Ti sheets were obtained.

Characterization. The morphology of laser-irradiated Ti surfaces was characterized by a Quantan 250 FEG scanning electron microscope (SEM, FEI, America) and a Flex 1000 SEM (Hitachi, Japan). The element content of the Ti sample was measured by an energy dispersive X-ray spectroscopy (EDXS). The crystal structures of the untreated and laser-irradiated Ti samples were analyzed with a powder X-ray diffractometer (XRD, Rigaku, Smartlab, Japan). The 3D and the cross-sectional profiles of the micro-patterns were observed by using a LEXT-OLS4000 laser confocal microscope (Olympus, Japan). The wettability of Ti surfaces was examined using a contact angle system (JC2000D4, Powereach, China). The volume of each water droplet is about 7 µL.

Fog collection test. The center of micro-patterned Ti sheets was faced to the nozzle of the humidifier, whose flow rate was about 0.2 cm³/s. The distance between as-prepared samples and the humidifier is 10 cm with a vertical incidence angle. A graduated cylinder was utilized to collect water droplets that slide from as-prepared sheets. The weight

of collected water was measured by a high-precision balance.

3. Results and discussion

A femtosecond laser is able to change the surface topography and chemical composition on the Ti surface. Fig. 2a shows the SEM image of the Ti surface after the line-by-line laser scanning process. Under the action of laser etching, plasma ejecting and recrystallization of ejected particles, abundant micro-protrusions are randomly formed on the surface. The diameter of protrusions is in the range of several microns to sub-microns, and each protrusion is modified with a great number of nanoparticles, which realize the hierarchical micro/nanostructures. During laser irradiation, the element contents of the Ti surface are also changed (Fig. 2b). EDXS result presents that the atomic proportion of O increases from 0% to 43.08% while the atomic proportion of Ti decreases to 56.92%. It can be seen that oxidized Ti occurs concurrently during laser etching and plasma ejecting. Since Ti⁴⁺ is a more stable state in metallic oxide, the resultant micro/nanostructures are composed of TiO₂ [36–38].

Pure Ti is a kind of hydrophilic material. As is shown in Fig. 2c, a water droplet on a flat Ti surface presents a water contact angle (WCA) of $64^{\circ} \pm 1^{\circ}$. After heat treatment and dark storage, the wettability remains hydrophilic with a WCA of $69.5^{\circ} \pm 1.5^{\circ}$. For laser-ablated samples, the hierarchical micro/nanostructures endow Ti surfaces with superhydrophilicity. A water droplet will entirely spread out when touching the surface (Fig. 2d). Surprisingly, the as-prepared surface is gradually hydrophobic upon dark storage. Finally, the WCA is found to be $157^{\circ} \pm 1^{\circ}$, which indicates that the laser-ablated surface is able to vary from superhydrophilicity to superhydrophobicity without any chemical treatment. The underlying mechanism of this phenomenon is resulted from the formation of TiO2, as is depicted in Fig. 2e. Femtosecond laser-induced hierarchical micro/nanostructures include abundant TiO2, which is a typical photocatalytic and hydrophilic material. During femtosecond laser microfabrication process, the valence bond surrounding Ti⁴⁺ is a highly unstable state, lattice oxygen interacts with holes generating electron-hole pairs, which is easy to react with H₂O and form Ti-OH groups. The combination of -OH groups and hierarchical micro/nanostructures amplifies its hydrophilicity. It is worth mentioning that Ti-OH groups are easily lost in the dark. Heat treatment is able to accelerate this process. After being stored in an opaque oven at 100°C for 24 h, -OH groups on the laser-ablated samples are gradually replaced by -O groups and other oxides with low surface energy. Hence, the presence of low surface energy groups and hierarchical micro/ nanostructures endows the resultant surface with superhydrophobicity.

Through heat treatment and dark storage, the laser-ablated area on Ti surface obtains superhydrophobic ability while the flat area remains

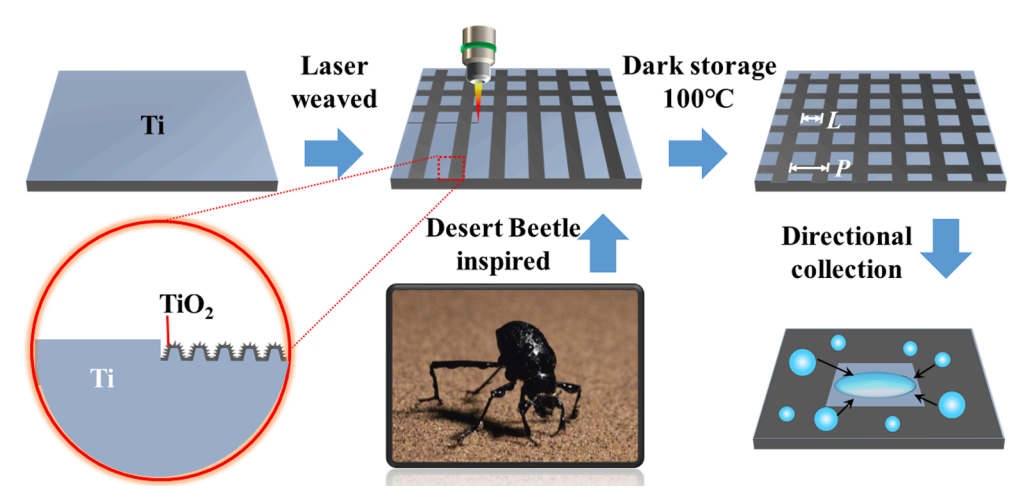


Fig. 1. The schematic of femtosecond laser weaving process on a Ti surface for water harvesting.

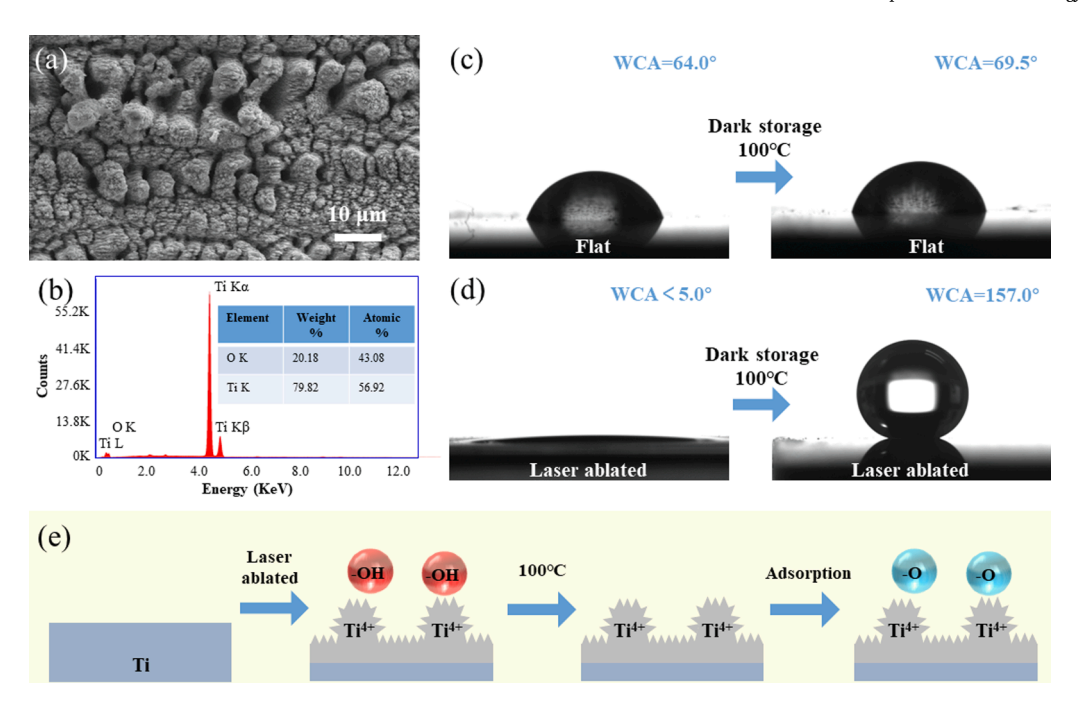


Fig. 2. (a) SEM image of the laser-ablated Ti surface. (b) EDXS result of the laser-ablated Ti surface. (c) The wettability of untreated Ti surface before and after dark storage. (d) The wettability of laser-ablated Ti surface before and after dark storage. (e) Schematic illustration of the variation from hydrophilicity to superhydrophobicity via laser ablation and heat treatment.

hydrophilic. Hence, hybrid superhydrophobic/hydrophilic patterns on Ti surfaces are able to realize via femtosecond laser selectively ablation. The morphology of the laser-ablated hybrid pattern is depicted in Fig. 3a and Fig. 3b. P is set as 300 μ m and L is programmed to 240 μ m. A uniform square array is formed by femtosecond laser weaving process (Fig. 3c). The width (W) of laser irradiated micro-groove is 60 μ m and its depth is about 12 μ m. Further magnified SEM image presents that abundant nanoparticles with the size of 50 nm to 500 nm are decorated on the groove (Fig. 3d).

As shown in Fig. 3f, localized XRD results on square arrays and pure Ti are almost entirely the same. On laser irradiated micro-groove, the peaks of Ti(110), Ti(101), Ti(210), Ti(220) are detected and the peaks of Ti(111) and Ti(310) are also significantly enhanced, indicating the formation of TiO_2 . According to Fig. 2c and Fig. 2d, flat Ti surfaces

endow square arrays with hydrophilicity while rough ${\rm TiO_2}$ particles endow microgrooves with superhydrophobicity after dark storage. Besides, ejected particles not only recrystallizes on the microgroove but also the edge of the untreated area. The size and number of eject nanoparticles decrease with the increasing distance (Fig. 3e). Owing to the different wettability of ${\rm TiO_2}$ nanoparticles and flat Ti substances, the wettability gradually varies from superhydrophobicity to hydrophilicity with the decreasing of recrystallized nanoparticles. Hence, the laser-induced square array pattern can be divided into three parts: superhydrophobic area, hydrophilic area, and transitional area, as shown in Fig. 3e. The existence of the transitional area forms a gradient wetting and a wetting driving force, which is more beneficial to the transport of water droplets.

Inspired by desert beetles, the as-prepared hydrophilic/

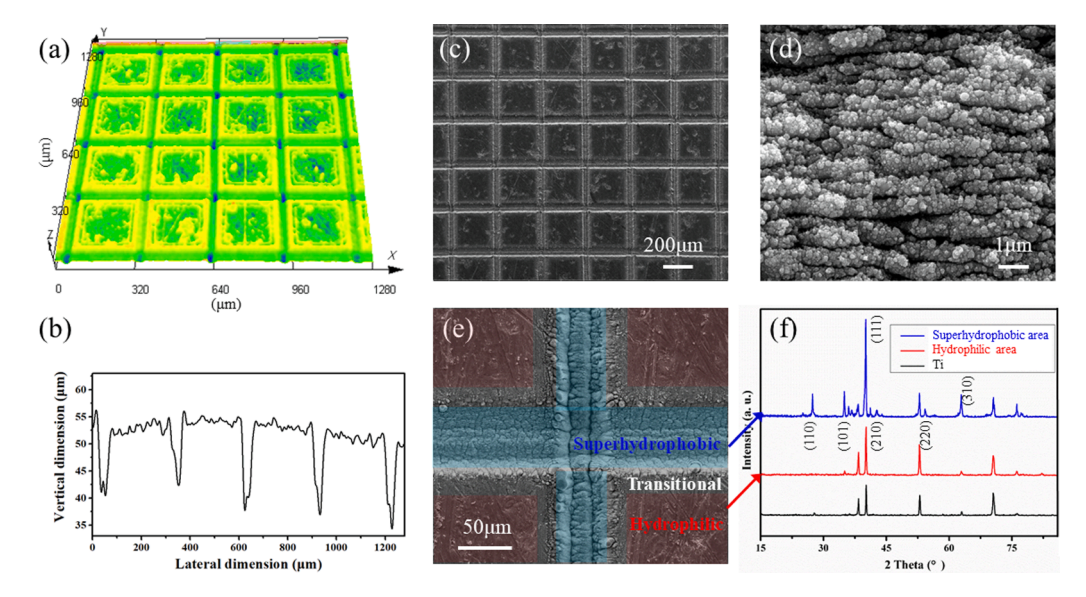


Fig. 3. (a) 3D confocal microscopy image of the as-prepared square array pattern; (b) Cross-sectional profiles of the as-prepared square array pattern. (c-e) SEM image of the as-prepared square array pattern. (f) XRD results of superhydrophobic area, hydrophilic area, and pure Ti.

superhydrophobic samples are applied to collect fog in air. As controls, untreated Ti sheets are chosen as hydrophilic samples and line-by-line laser-structured Ti sheets are named superhydrophobic samples. A commercial humidifier was applied to analyze the fog collection efficiency of the above-mentioned samples. After 30 s, water mist is already condensed into micro-droplets and spread out on the hydrophilic sample. Nevertheless, the water drop does not tend to slide off owing to the high surface adhesion (Fig. 4a). On the superhydrophobic sample, water mist is hard to capture and its water collection rate is inefficient. Comparatively, the as-prepared sample shows a high efficiency of water collection. A water droplet array occurs on the square array uniformly while the rest of the surface remains dry. With the growth of water droplets and the limitation of superhydrophobic edge, condensate water is easy to slide down and detach the as-prepared surfaces, realizing the collection of water mist in air. In the first 40 min, the collecting efficiency of the superhydrophobic samples is measured higher than hydrophilic ones because much-collected water is still spread out on the hydrophilic surface. As exhibited in Fig. 4b, the collected water of hydrophilic samples, superhydrophobic samples, and as-prepared samples is about 580 mg/cm², 620 mg/cm², and 1100 mg/cm² respectively after 1 h. With the increase of time, the collection rate of the as-prepared samples is holding at 1350 mg/cm² h, which is nearly twice as hydrophilic samples and three times as superhydrophobic samples in the final.

The key of water collection rate can be divided into two parts: capture and transportation. When water mist comes into contact with the superhydrophobic sample, most of the water mist bounces off and repels from the superhydrophobic surfaces, indicating the inefficiency of water capturing. Although the water flow can be successfully captured by hydrophilic and superhydrophilic surfaces, the water will quickly spread out and form a water membrane on the whole surface. The obtained water membrane is not only difficult to transport but also prevents further contact between water mist and sample surfaces, leading to low efficiency of collection rate. Compared to these samples, the collection efficiency is greatly improved via femtosecond laser weaving hybrid pattern. Hydrophilic square arrays are applied to capture water mist in air and superhydrophobic microgrooves reduce the contact area between captured droplets and sample surfaces. The transition area provides a wetting gradient force that helps captured droplets converge in

square arrays better. Meanwhile, the regular pattern causes water droplets to be arranged in a square array, which is a benefit to their regular and orderly transportation. Hence, water drops can be transported and slide down with a smaller volume and a less time cost.

The hybrid hydrophilic/superhydrophobic surfaces with different W were also discussed, as shown in Fig. 4c. When W is controlled from 60 μ m to 80 μ m, the efficiency of the collection rate is significantly enhanced. As W continues to increase, hydrophilic square arrays are too small to capture enough water. On the contrary, superhydrophobic barriers are difficult to form when W is small than 40 μ m. Furthermore, the influence of P is also investigated in Fig. 4d. 3D confocal microscopy image of the as-prepared square array pattern with different P is shown in Figure S2. With increasing P, The captured water on sample surfaces increases while the transportability of water droplets becomes weaker. Considering the balance between water capture and transport, the sample with $P=300~\mu$ m and $W=60~\mu$ m leads to the highest efficiency of collection rate.

It is worth mentioning that the ratio of the laser structured area is only 36% on the whole surface so that the processing efficiency is also improved compared with the existing femtosecond laser scanning technology. As shown in Figure S3, a larger superhydrophobic/ hydrophilic surface can also be fabricated by femtosecond select weaving process. Furthermore, compared to other femtosecond laser-induced water-collecting devices, the whole process does not need chemical modification and any fluoride, which is more suitable to meet the ecofriendly rules (Table 1).

4. Conclusions

In summary, a hybrid superhydrophobic/hydrophilic Ti surface for water harvesting was prepared by femtosecond laser weaving process and dark storage. During femtosecond laser selectively ablation, rough ${\rm TiO_2}$ micro/nanostructures were formed on laser-scanned area, presenting superhydrophobicity, while untreated area remained intrinsic hydrophilicity. By adjusting the width and ratio of laser-ablated area, the efficiency of the water collection rate could be influenced significantly. When W and P were controlled as 60 μ m and 300 μ m, the water collection rate was optimized as 1400 mg·h/cm², which was twice as

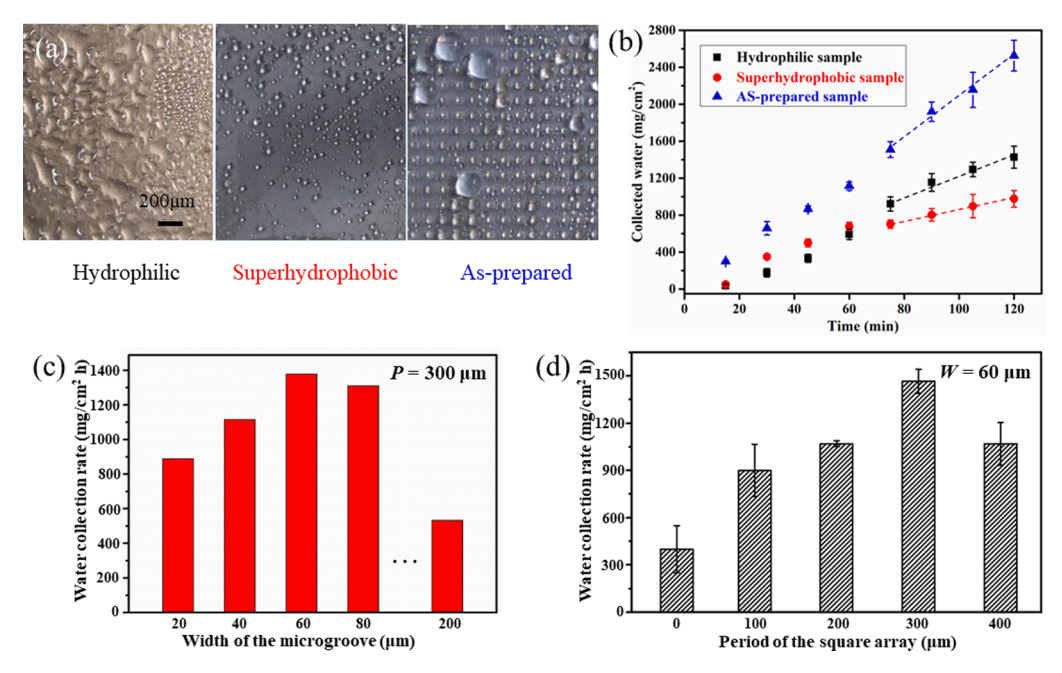


Fig. 4. (a) Optical image of water harvest results of hydrophilic, superhydrophobic, and as-prepared samples. (b) The variation of collected water for different samples along with the collection time. (c) Water-collection efficiency of the as-prepared samples with different *L*. (d) Water-collection efficiency of the as-prepared samples with different *P*.

Table 1An overview of femtosecond laser-induced fog/water collection surfaces.

Surface structures	Laser Processing	Chemical modification	Reference
Venation network	Overall scanning	PTFE	31
Janus membrane	Laser drilling and overall scanning	fluoroalkylsilane	32
Leaf veins	Overall scanning and selective scanning	fluoroalkylsilane	33
Nanoneedle structures	Overall scanning	NaOH, HCl, PDMS	34
Square array	Selective scanning	None	Our method

untreated Ti surface. Compared to other laser-induced water collection devices, our method exhibited a faster processing speed and did not need any chemical modification. We believe that this fast and eco-friendly method will make a new contribution to solving the shortage of water resources in the future.

CRediT authorship contribution statement

Jingzhou Zhang: Writing – original draft, Conceptualization, Methodology. **Yuanchen Zhang:** Data curation. **Jiale Yong:** Methodology, Writing – review & editing. **Xun Hou:** Resources. **Feng Chen:** Resources, Writing – review & editing.

Declaration of Competing Interest

The authors declare that they have no known competing financial interests or personal relationships that could have appeared to influence the work reported in this paper.

Acknowledgments

This work is supported by the National Science Foundation of China under the Grant nos. 61875158, the National Key Research and Development Program of China under the Grant no.2017YFB1104700, the International Joint Research Laboratory for Micro/Nano Manufacturing and Measurement Technologies, the Fundamental Research Funds for the Central Universities.

Appendix A. Supplementary data

Supplementary data to this article can be found online at https://doi.org/10.1016/j.optlastec.2021.107593.

References

- [1] J.T. Overpeck, Climate science: the challenge of hot drought, Nature 503 (2013) 350–351.
- [2] H. Yang, J.R. Thompson, R.J. Flower, Beijing 2022: olympics will make water scarcity worse, Nature 525 (2015) 455.
- $[3] \ \ https://baijiahao.baidu.com/s?id=1685401647883753233\&wfr=spider\&for=pc.$
- [4] M.M. Mekonnen, A.Y. Hoekstra, Four billion people facing severe water scarcity, Sci. Adv. 2 (2) (2016) e1500323, https://doi.org/10.1126/sciadv.1500323.
- [5] H. Zhu, F. Yang, J. Li, Z. Guo, High-efficiency water collection on biomimetic material with superwettable patterns, Chem. Commun. 52 (84) (2016) 12415–12417.
- [6] Y. Sun, Z. Guo, Recent advances of bioinspired functional materials with specific wettability: from nature and beyond nature. Nanoscale Horiz. 4 (1) (2019) 52–76.
- [7] X. Liu, F. Yang, J. Guo, J. Fu, Z. Guo, New insights into unusual droplets: from mediating the wettability to manipulating the locomotion modes, Chem. Commun. 56 (2020) 14757–14788.
- [8] S. Gam-Derouich, J. Pinson, A. Lamouri, P. Decorse, S. Bellynck, R. Herbaut, L. Royon, C. Mangeney, Micro-patterned anti-icing coatings with dual hydrophobic/hydrophilic properties, J. Mater. Chem. A 6 (40) (2018) 19353–19357.
- [9] Y. Wang, X. Wang, C. Lai, H. Hu, Y. Kong, B. Fei, J.H. Xin, Biomimetic watercollecting fabric with light-induced superhydrophilic bumps, ACS Appl. Mater. Interfaces 8 (5) (2016) 2950–2960.

- [10] H. Bai, C. Zhang, Z. Long, H. Geng, T. Ba, Y. Fan, C. Yu, K. Li, M. Cao, L. Jiang, A hierarchical hydrophilic/hydrophobic cooperative fog collector possessing selfpumped droplet delivering ability, J. Mater. Chem. A 6 (42) (2018) 20966–20972.
- [11] H. Kim, S.R. Rao, E.A. Kapustin, L. Zhao, S. Yang, O.M. Yaghi, E.N. Wang, Adsorption-based atmospheric water harvesting device for arid climates, Nat. Commun. 9 (2018) 1191.
- [12] M. Cao, J. Ju, K. Li, S. Dou, K. Liu, L. Jiang, Facile and large-scale fabrication of a cactus-inspired continuous fog collector, Adv. Funct. Mater. 24 (21) (2014) 3235–3240.
- [13] J. Ju, X.i. Yao, S. Yang, L. Wang, R. Sun, Y. He, L. Jiang, Cactus stem inspired conearrayed surfaces for efficient Fog collection, Adv. Funct. Mater. 24 (44) (2014) 6933–6938.
- [14] H. Chen, P. Zhang, L. Zhang, H. Liu, Y. Jiang, D. Zhang, Z. Han, L. Jiang, Continuous directional water transport on the peristome surface of nepenthes alata, Nature 532 (7597) (2016) 85–89.
- [15] J. Ju, H. Bai, Y. Zheng, T. Zhao, R. Fang, L. Jiang, A multi structural and multifunctional integrated fog collection system in cactus, Nat. Commun. 3 (2012) 1247.
- [16] J. Lin, X. Tan, T. Shi, Z. Tang, G. Liao, Leaf vein-inspired hierarchical wedgeshaped tracks on flexible substrate for enhanced directional water collection, ACS Appl. Mater. Interfaces 10 (51) (2018) 44815–44824.
- [17] N. Thakur, A.S. Ranganath, K. Agarwal, A. Baji, Electrospun bead-on-string hierarchical fibers for fog harvesting application, Macromol. Mater. Eng. 302 (7) (2017) 1700124, https://doi.org/10.1002/mame.v302.710.1002/ mame.201700124.
- [18] W. Shi, M.J. Anderson, J.B. Tulkoff, B.S. Kennedy, J.B. Boreyko, Fog harvesting with harps, ACS Appl. Mater. Interfaces 10 (14) (2018) 11979–11986.
- [19] S.H. Lee, J.H. Lee, C.W. Park, C.Y. Lee, K. Kim, D. Tahk, M.K. Kwak, Continuous fabrication of bio-inspired water collecting surface via roll-type photolithography, Int. J. Precis. Eng. Manuf. 1 (2014) 119–124.
- [20] J. Zhang, K. Zhang, J. Yong, Q. Yang, Y. He, C. Zhang, X. Hou, F. Chen, Femtosecond laser preparing patternable liquid-metal-repellent surface for flexible electronics, J. Colloid Interface Sci. 578 (2020) 146–154.
- [21] J. Zhang, J. Yong, C. Zhang, K. Zhang, Y. He, Q. Yang, X. Hou, F. Chen, Liquid metal-based reconfigurable and repairable electronics designed by a femtosecond laser, ACS Appl. Electron. Mater. 2 (8) (2020) 2685–2691.
- [22] H. Wu, L. Zhang, S. Jiang, Y. Zhang, Y. Zhang, C. Xin, S. Ji, W. Zhu, J. Li, Y. Hu, D. Wu, J. Chu, Ultrathin and high-stress-resolution liquid-metal-based pressure sensors with simple device structures, ACS Appl. Mater. Interfaces 12 (49) (2020) 55390–55398.
- [23] J. Zhang, J. Yong, Q. Yang, F. Chen, X. Hou, Femtosecond laser-induced underwater superoleophobic surfaces with reversible pH-responsive wettability, Langmuir 35 (9) (2019) 3295–3301.
- [24] J. Yong, F. Chen, Q. Yang, D. Zhang, G. Du, J. Si, F. Yun, X. Hou, Femtosecond laser weaving superhydrophobic patterned PDMS surfaces with tunable adhesion, J. Phys. Chem. C 117 (47) (2013) 24907–24912.
- [25] J. Yong, Y. Fang, F. Chen, J. Huo, Q. Yang, H. Bian, G. Du, X. Hou, Femtosecond laser ablated durable superhydrophobic PTFE films with micro-through-holes for oil/water separation: Separating oil from water and corrosive solutions, Appl. Surf. Sci. 389 (2016) 1148–1155.
- [26] J. Wu, J. He, K. Yin, Z. Zhu, S.i. Xiao, Z. Wu, J.-A. Duan, Robust hierarchical porous PTFE film fabricated via femtosecond laser for self-cleaning passive cooling, Nano Lett. 21 (10) (2021) 4209–4216.
- [27] Y. Fang, J. Yong, F. Chen, J. Huo, Q. Yang, J. Zhang, X. Hou, Bioinspired fabrication of bi/tridirectionally anisotropic sliding superhydrophobic PDMS surfaces by femtosecond laser, Adv. Mater. Interfaces 5 (2018) 1701245.
- [28] K. Yin, Z. Wu, J. Wu, Z. Zhu, F. Zhang, J. Duan, Solar-driven thermal-wind synergistic effect on laser-textured superhydrophilic copper foam architectures for ultrahigh efficient vapor generation, Appl. Phys. Lett. 118 (2021), 211905.
- [29] K. Yin, D. Chu, X. Dong, C. Wang, J.-A. Duan, J. He, Femtosecond laser induced robust periodic nanoripple structured mesh for highly efficient oil-water separation, Nanoscale 9 (37) (2017) 14229–14235.
- [30] E. Kostal, S. Stroj, S. Kasemann, V. Matylitsky, M. Domke, Fabrication of biomimetic fog-collecting superhydrophilic-superhydrophobic surface micropatterns using femtosecond lasers, Langmuir 34 (9) (2018) 2933–2941.
- [31] K. Yin, H. Du, X. Dong, C. Wang, J.-A. Duan, J. He, A simple way to achieve bioinspired hybrid wettability surface with micro/nanopatterns for efficient fog collection, Nanoscale 9 (38) (2017) 14620–14626.
- [32] F. Ren, G. Li, Z. Zhang, X. Zhang, H. Fan, C. Zhou, Y. Wang, Y. Zhang, C. Wang, K. Mu, Y. Su, D. Wu, A single-layer Janus membrane with dual gradient conical micropore arrays for self-driving fog collection, J. Mater. Chem. A 5 (35) (2017) 18403–18408.
- [33] W. Liu, P. Fan, M. Cai, X. Luo, C. Chen, R. Pan, H. Zhang, M. Zhong, An integrative bioinspired venation network with ultra-contrasting wettability for large-scale strongly self-driven and efficient water collection, Nanoscale 11 (18) (2019) 8940–8949.
- [34] J. Lu, C.-V. Ngo, S.C. Singh, J. Yang, W. Xin, Z. Yu, C. Guo, Bioinspired hierarchical surfaces fabricated by femtosecond laser and hydrothermal method for water harvesting, Langmuir 35 (9) (2019) 3562–3567.
- [35] Y. Jiao, C. Li, S. Wu, Y. Hu, J. Li, L. Yang, D. Wu, J. Chu, Switchable underwater bubble wettability on laser-induced titanium multiscale micro-/nanostructures by vertically crossed scanning, ACS Appl. Mater. Interfaces 10 (19) (2018) 16867–16873.
- [36] C. Zhou, G. Li, C. Li, Z. Zhang, Y. Zhang, S. Wu, Y. Hu, W. Zhu, J. Li, J. Chu, Z. Hu, D. Wu, L. Yu, Three-level cobblestone-like TiO₂ micro/nanocones for dual-

- responsive water/oil reversible wetting without fluorination, Appl. Phys. Lett. 111
- (2017), 141607.
 [37] S. Ye, Q. Cao, Q. Wang, T. Wang, Q. Peng, A highly efficient, stable, durable, and recyclable filter fabricated by femtosecond laser drilling of a titanium foil for oil-water separation, Sci. Rep. 6 (2016) 37591.
- [38] J. Yong, F. Chen, Q. Yang, U. Farooq, X. Hou, Photoinduced switchable underwater superoleophobicity-superoleophilicity on laser modified titanium surfaces, J. Mater. Chem. A 3 (20) (2015) 10703–10709.